Available online at www.sciencedirect.com
SCIENCE DIRECT®
Journal of Non-Crystalline Solids 331 (2003) 240–253
JOURNAL OF NON-CRYSTALLINE SOLIDS
www.elsevier.com/locate/jnoncrysol

Mutant crystals in $Na_2O \cdot 2CaO \cdot 3SiO_2$ glasses

V.M. Fokin [a,1], O.V. Potapov [b], E.D. Zanotto [a,*], F.M. Spiandorello [a], V.L. Ugolkov [b], B.Z. Pevzner [b]

[a] *Department of Materials Engineering, Vitreous Materials Laboratory, Federal University of São Carlos, São Carlos, SP 13565-905, Brazil*

[b] *Institute of Silicate Chemistry, Russian Academy of Sciences, Odoevskogo 24/2, St. Petersburg 199155, Russia*

Received 6 January 2003

Abstract

This paper presents strong evidence for a continuous variation in glass and crystal compositions during crystallization, from the early stages of nucleation up to full transformation of a stoichiometric $Na_2O \cdot 2CaO \cdot 3SiO_2$ glass, as well as of similar glasses that are depleted or enriched in sodium. During crystallization, the crystal compositions approach those of the parent glasses, leading to the inference that the critical clusters were also sodium-enriched. The existence of such mutant crystals is reported for the first time. The crystals' increase in sodium content diminishes the thermodynamic barrier for nucleation owing to a decrease in the critical nucleus/liquid interfacial energy. This conclusion is evident also from an analysis of the nucleation rate as a function of the glass composition. Our conclusions are based on the analysis of a plethora of data: overall crystallization kinetics, crystal growth velocity, changes in the crystal's lattice parameters, variation of the reversible polymorphic transition temperature with the degree of crystallinity and, finally, quantitative measurements of glass and crystal composition by EDS. The deviation of the nucleus composition from the expected stoichiometry may significantly impact the analysis of nucleation theories.

1. Introduction

When any vitreous material is heated for a long enough time above the glass transition temperature, T_g, crystallization readily starts from surface or internal nuclei. Nucleation is thus a key step for both controlled and spontaneous crystallization (devitrification). However, relevant experimental tests of the classic nucleation theory (CNT) have demonstrated its failure to quantitatively describe nucleation rates. If one assumes a constant nucleus/liquid surface energy and uses either the viscosity or the induction time to account for the molecular rearrangements at the nucleus/matrix interface, drastic discrepancies result between theoretical and experimental nucleation rate values, regardless of the expression used to estimate the driving force.

Some possible explanations so far advanced for the CNT failure are: (i) metastable phase precipitation in the early stages of nucleation; (ii) a

* Corresponding author. Tel.: +55-16 271 4871; fax: +55-16 261 5404.
E-mail address: dedz@power.ufscar.br (E.D. Zanotto).
[1] On sabbatical leave from S.I. Vavilov's State Optical Institute, Babushkina 36/1, St. Petersburg 193171, Russia.

0022-3093/$ - see front matter © 2003 Elsevier B.V. All rights reserved.
doi:10.1016/j.jnoncrysol.2003.08.074

possible dependence of the surface energy on temperature and nucleus size and (iii) elastic strain effects due to the difference of specific volumes of crystal and glass [1–12]. In this paper we will focus on a new possibility, i.e. on the nature of the first phase to nucleate – precipitation of a solid solution of varying composition.

In order to apply any nucleation theory to the analysis of experimental nucleation rates in undercooled liquids, one must first identify what phase crystallizes out. Owing to small size of the critical nuclei, this is not a trivial problem. The existing methods to estimate nucleation rates are indirect and, typically, micrometric crystals can only be detected and counted after the nuclei have grown from their original critical size of a few nanometers.

To test nucleation and crystal growth theories, stoichiometric glasses are often used as model systems. In doing so, it is assumed that the evolving macrocrystals and the critical nucleus belong to the same crystallographic phase and have the *same* composition as the parent glass. In this approximation, stoichiometric glasses are considered 'single-component' systems. However, according to Ostwald's rule of stages "...in the course of transformation of an unstable (or metastable) state into a stable one, the system does not go *directly* to the most stable conformation – corresponding to the modification with the lowest free energy – but prefers to reach intermediate stages (corresponding to other possible metastable modifications) having the closest free energy difference to the initial state" [1].

Solid arguments were recently put forward in favor of the nucleation of a metastable phase as a primary phase in lithium disilicate glass [2]. That study stimulated the search for metastable phases by direct methods [3–6], confirming their precipitation in the early stages of crystallization. It should be stressed that lithium disilicate glass has served as a model to study homogeneous nucleation for several years [7–10] because this is one of the few stoichiometric silicate glasses showing volume nucleation without the use of surfactants or crystallization cores.

Stoichiometric $Na_2O \cdot 2CaO \cdot 3SiO_2$ glass also belongs to this family of glass-forming melts that show internal nucleation [13–15]. We have previously demonstrated that crystals grown in this stoichiometric glass at high temperatures dramatically hinder the formation of new crystals at low temperatures in their vicinity [16]. This effect was dubbed the 'courtyard' phenomenon. Additionally, we observed a decrease in the crystal growth velocity with increasing heat treatment time or increasing crystallinity. The first EDS measurements indicated that the above-mentioned facts are caused by a difference in composition between glass and evolving solid solution crystals [16,17]. The formation of solid solutions is consistent with the phase diagram of a pseudo binary section $CaO \cdot SiO_2$–$Na_2O \cdot SiO_2$ [18].

This paper presents strong new evidence for a continuous variation in glass and crystal compositions during crystallization, from the early stages of nucleation up to full transformation of a stoichiometric glass $Na_2O \cdot 2CaO \cdot 3SiO_2$ glass, as well as of similar glasses that are depleted or enriched in Na. Our conclusions are based on the analysis of a plethora of data: overall crystallization kinetics, crystal growth velocity, changes in the crystal's lattice parameters, variation of the reversible polymorphic transition temperature with the degree of crystallinity and, finally, quantitative measurements of glass and crystal composition by EDS. To visualize areas of glass with modified compositions, we used special double-stage heat treatments.

2. Materials and methods

The same glasses used in [15,16] were employed in this study. The glass compositions, which are shown in Table 1 and in the composition triangle, Fig. 1, are close to the line of constant $CaO/SiO_2 = 2/3$ ratio. The composition of glass N4 is the closest to the stoichiometric one, which is denoted by an open star. The degree of crystallinity was measured with both optical microscopy (Neophot) and X-ray analysis (DRON-2). The unit-cell parameters of the solid solution crystals were calculated from the X-ray diffraction spectra of fully and partially

Table 1
Glass compositions by analysis (mol%)

Glass	Na_2O	CaO	SiO_2
N1	15	34.1	50.9
N2	15.5	33.8	50.7
N3	16.4	33.3	50.3
N4	17	33.2	49.8
N5	18.6	32.5	48.9
NC_2S_3[a]	16.67	33.33	50.00

[a] Nominal stoichiometric composition: $Na_2O \cdot 2CaO \cdot 3SiO_2$.

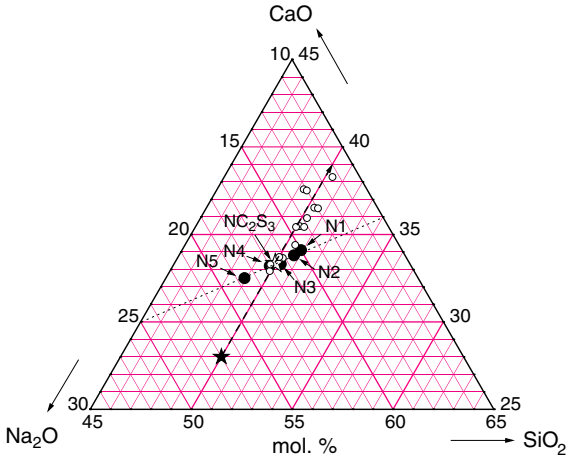

Fig. 1. Positions of glasses on the composition triangle. Black circles indicate the positions of glasses N1–N5. Open star refers to the stoichiometric composition $Na_2O \cdot 2CaO \cdot 3SiO_2$ (NC_2S_3). Black star refers to the initial composition of the crystal nuclei in glass N4. Opened circles show the compositional variation of the glass matrix during crystallization of glass N4. Dot line corresponds to constant concentrations ratio $CaO/SiO_2 = 2/3$. Dash line is the pseudo-binary cut $Na_2O \cdot SiO_2$–$CaO \cdot SiO_2$.

crystallized glasses. Germanium was used as an internal standard.

Well below the glass transition temperature, solid solution crystals undergo a reversible polymorphic transition at a temperature T_{pm}, which is very sensitive to their compositional changes. This reversible polymorphic transition is accompanied by a heat effect and a change in the volume of the unit-cell [19,20]. DSC runs and dilatometry were used to estimate T_{pm}.

The crystal and glass compositions were estimated by energy dispersive spectroscopy (EDS), using glass and crystal samples with known compositions as references.

3. Results

3.1. Overall crystallization kinetics

Figs. 2–4 present the variations of the volume fraction crystallized (a, b) and the sizes of the largest crystals (c, d) with increasing heat treatment time at 590 °C (Fig. 2), 650 °C (Fig. 3) and 720 °C (Fig. 4) for glass N4 (composition very close to stoichiometry). Similar plots for glasses depleted (N1) and enriched (N5) in Na are given in Figs. 5 and 6, respectively. The heat treatment temperatures are indicated by arrows in Fig. 7 to demonstrate their position relative to that of the nucleation rate maximum. The crystals in glass N1 have an almost spherical morphology, but are cube-shaped in glasses N4 and N5.

3.2. Variations of crystal cell parameters and temperature of reversible polymorphic transition

Fig. 8 shows parameter ***a*** of the hexagonal cell of the solid solution crystals as a function of Na_2O content, C_{Na_2O}, for fully crystallized glasses (a) and the volume fraction of crystals, α, for partially crystallized glasses (b–f).

The values of T_{pm} as a function of C_{Na_2O} (for fully crystallized glasses) and of α (for partially crystallized glass N4) are given in Figs. 9 and 10, respectively.

3.3. Evolution of crystal and glass composition during crystallization

Measurements of Na, Ca, Si and O content were performed by EDS for samples of glass N4 subjected to heat treatments at $T = 650$ and 720 °C marked in Fig. 7. Figs. 11 and 12 present these data versus α. For the heat treatment at $T = 650$ °C (producing a crystal size distribution owing to simultaneous nucleation and growth), only the glass composition was measured while, in the case of the heat treatment at $T = 720$ °C (growth of a constant number of 'athermic' crystals), the crystal composition was measured.

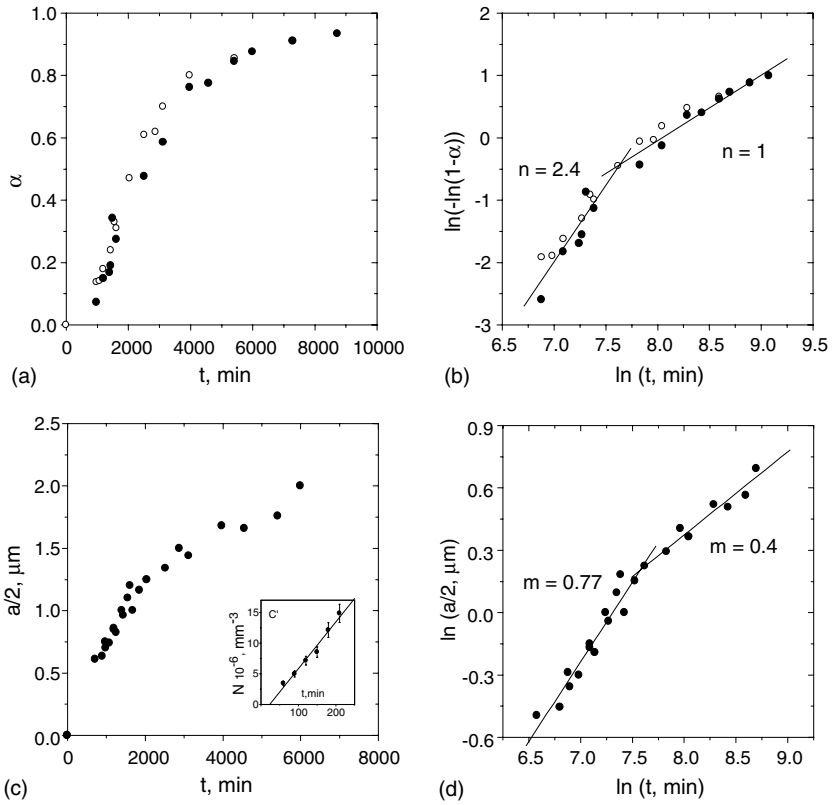

Fig. 2. Volume fraction of crystals (a, b), size of the largest crystals (c, d), and number of crystals (c′) as functions of the heat treatment time at $T = 590$ °C for glass N4. Open circles – X-ray analysis; closed circles – optical microscopy. Solid lines are linear fit.

3.4. The 'courtyard' phenomenon

Fig. 15 presents scanning electron microscopy (SEM) micrographs of glass samples (N1, N4 and N5) subjected to single-stage heat treatments at a temperature T_{n-g} (a, c, e), and to double-stage heat treatments (b, d, f): first at a temperature T_{gr} ($T_{gr} > T_{n-g}$), corresponding to a sufficiently high crystal growth rate, and then at the same temperature T_{n-g} for the same time as the samples in Fig. 15(a, c, e).

4. Discussion

Analyses of overall crystallization kinetics are often based on the Johnson–Mehl–Avrami–Kolmogorov (JMAK) equation [21]

$$\alpha(t) = 1 - \exp\left\{ - c_g \int_0^t I(t') \left[\int_{t'}^t U(t'')\,dt'' \right]^d dt' \right\}, \tag{1}$$

where α is the volume fraction transformed (crystallized), c_g is a shape factor, d is the dimensionality of growth, and I and U are the nucleation and growth rates. If I and U are constant, Eq. (1) can be written as

$$\alpha(t) = 1 - \exp\left\{ - \frac{c_g I U^3 t^4}{4} \right\}. \tag{2}$$

If, in the course of phase transformation, the number of new phase particles (crystals) does not vary and is equal to N_0 the volume fraction $\alpha(t)$ is given by Eq. (3):

$$\alpha(t) = 1 - \exp\left\{ - c_g N_0 U^3 t^3 \right\}. \tag{3}$$

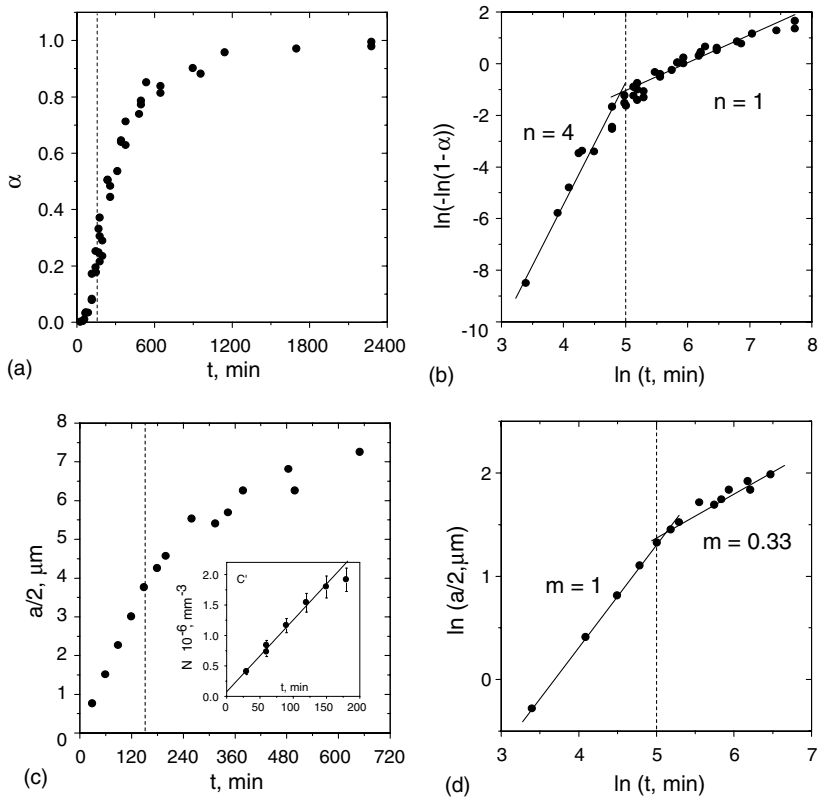

Fig. 3. Volume fraction of crystals (a, b), size of the largest crystals (c, d), and number of crystals (c′) as functions of the heat treatment time at $T = 650$ °C for glass N4. Solid lines are linear fit.

Eqs. (2) and (3) assume three-dimensional growth ($d = 3$).

Avrami proposed the use of the following general relationship:

$$\alpha(t) = 1 - \exp\{-Kt^n\}, \tag{4}$$

where n, the so-called Avrami coefficient, can have different values depending on the mechanism of nucleation and growth. The coefficient n can be estimated from the slope of the $\ln[-\ln(1-\alpha(t))]$ versus $\ln(t)$ plot.

Eq. (4) is valid in most cases of constant growth rate, and is approximately valid for the early stages of diffusion-controlled growth [22]. We therefore use this equation for a preliminary view of the transformation course. For three-dimensional growth, the Avrami coefficient can be written as

$$n = \kappa + 3m, \tag{5}$$

where κ and m are taken from the formulas $N \sim t^{\kappa}$ and $R \sim t^m$ describing the variation of the crystal number (N) and size (R) over time. Using the values n and m from the experimental dependences $\alpha(t)$ and $R(t)$, one can calculate the value of κ, thereby obtaining information about the nucleation process.

Figs. 2–6 present the overall crystallization and the growth kinetics. At every heat treatment temperature, the crystal growth rate in the glass of stoichiometric composition (N4), as well as in the glasses with shifted compositions (N1, N5), deviates considerably from a linear law (see Figs. 2–6(c, d)), evidencing the fact that crystal growth is controlled mainly by volume diffusion, and hence, that the crystal compositions are dissimilar to that of glass. It should be stressed that, in the present case, the crystals are solid solutions [20]. We will show later that their composition changes during growth, approach-

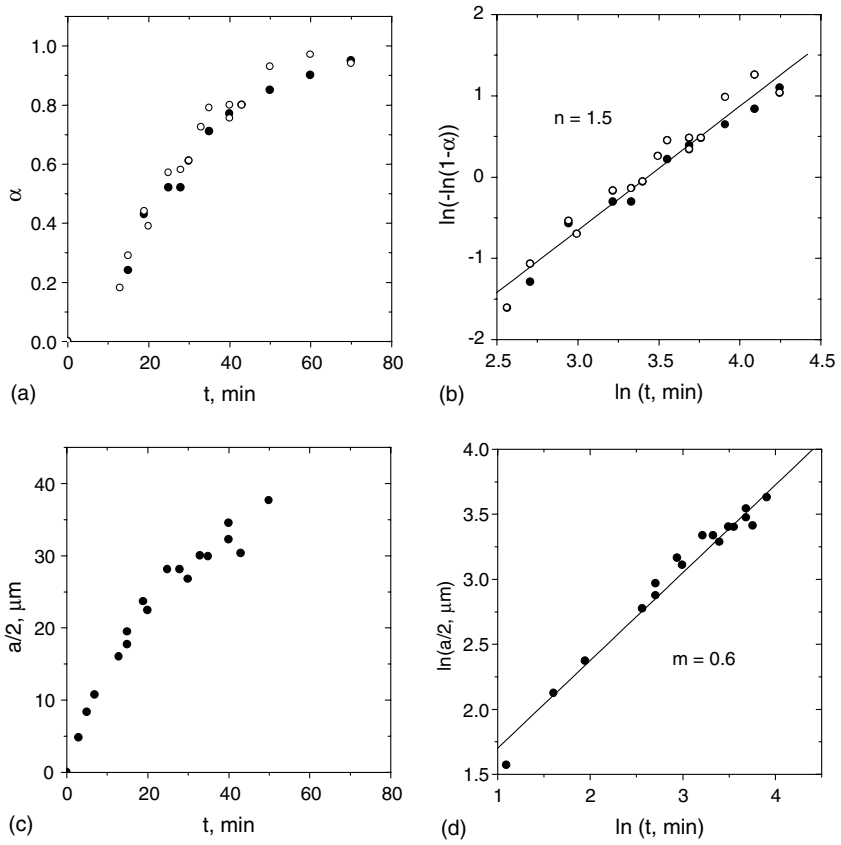

Fig. 4. Volume fraction of crystals (a, b) and size of the largest crystals (c, d) as functions of heat treatment time at $T = 720$ °C for glass N4. Open circles – X-ray analysis; closed circles – optical microscopy. Solid lines are linear fit.

ing the parent glass composition with increasing crystallized volume fraction. This fact partially explains the deviation of the coefficient m from 0.5 (see Table 2), which is typical for the diffusion-controlled growth [21] of a crystal of *constant* composition. Together with the coefficient m, which characterizes the growth kinetics, Table 2 shows the Avrami coefficients obtained from the $\ln[-\ln(1-\alpha(t))]$ versus $\ln(t)$ plots of Figs. 2–6.

The analysis of the overall crystallization kinetics indicated a time and temperature-related change in the crystallization mechanism. Fig. 2 and Table 2 show that, beginning at $t \sim 1000$ min, the increase of the crystallized volume fraction in glass N4 ('stoichiometric' composition) at $T = 590$ °C can be explained only by crystal growth ($n = 3m$) from a pre-determined number of nuclei. Hence, at the time of the first measurements of α ($t \sim 1000$ min), the number of crystals was already constant. Let us recall that $T = 590$ °C is very close to the temperature of the nucleation rate maximum (see Fig. 7). At $T = 650$ °C, nucleation takes place up to $t \sim 150$ min: $n \approx 1 + 3m$. Thus, at $t > 150$ min, as with $T = 590$ °C, the development of crystallinity, $\alpha(t)$, can be explained only by crystal growth: $n \approx 3m$ (see Fig. 3 and Table 2). A similar termination of nucleation follows from the overall crystallization kinetics of glass N5 at $T = 647$ °C (Fig. 6). The $N(t)$ plots (Figs. 2(c′), 3(c′) and 6(c′)) show the increase in the number of crystals over relatively short times. It should be noted that, in all the cases listed above, the crystallized volume does not exceed 20% at the moment when nucleation ceases.

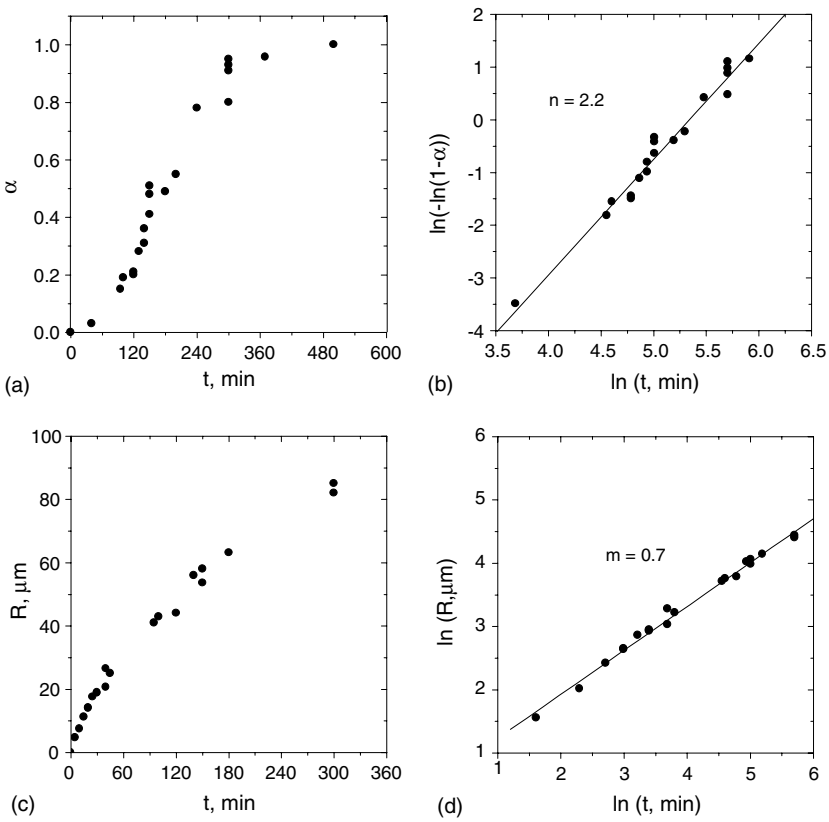

Fig. 5. Volume fraction of crystals (a, b) and size of the largest crystals (c, d) as functions of heat treatment time at $T = 700$ °C for glass N1. Solid lines are linear fit.

At $T = 720$ °C (glass N4) and $T = 700$ °C (glass N1), which are far from the nucleation rate maximum (see Fig. 7), the overall crystallization is governed only by crystal growth, as we expected.

Measurements of the crystal cell parameters give indirect evidence of the change in crystal and, correspondingly, glass compositions during crystallization. Fig. 8(a) shows the increase in the ***a*** parameter of the hexagonal crystal cell with increasing sodium content in the parent glass. These measurements refer to fully crystallized glasses. In this case, the crystal composition is clearly equal to that of the parent glass. The decrease in the ***a*** parameter is observed with increasing crystallized volume fraction α for both 'stoichiometric' glass N4 and glasses N1 and N5 (Fig. 8(b–f)), leading us to assume that, at the beginning of the phase transformation, the solid solution crystals contain more sodium than the fully crystallized glass.

The strong variation of the reversible polymorphic transition temperature, T_{pm}, also indicates a change in the crystal composition. According to Fig. 9, the smaller the sodium content in the crystals (fully crystallized glasses), the greater the T_{pm}. Hence, we may attribute the increase in T_{pm} with increasing α in the partly crystallized glass N4 (Fig. 10) to the decrease in the crystals' sodium oxide content.

The above-described experimental facts were explained by a variation of the compositions of both solid solution crystals and glass in the course of phase transformation. Indeed, direct measurements by EDS confirmed this assumption. According to Fig. 11, the sodium content in the glass matrix decreases and the calcium content increases

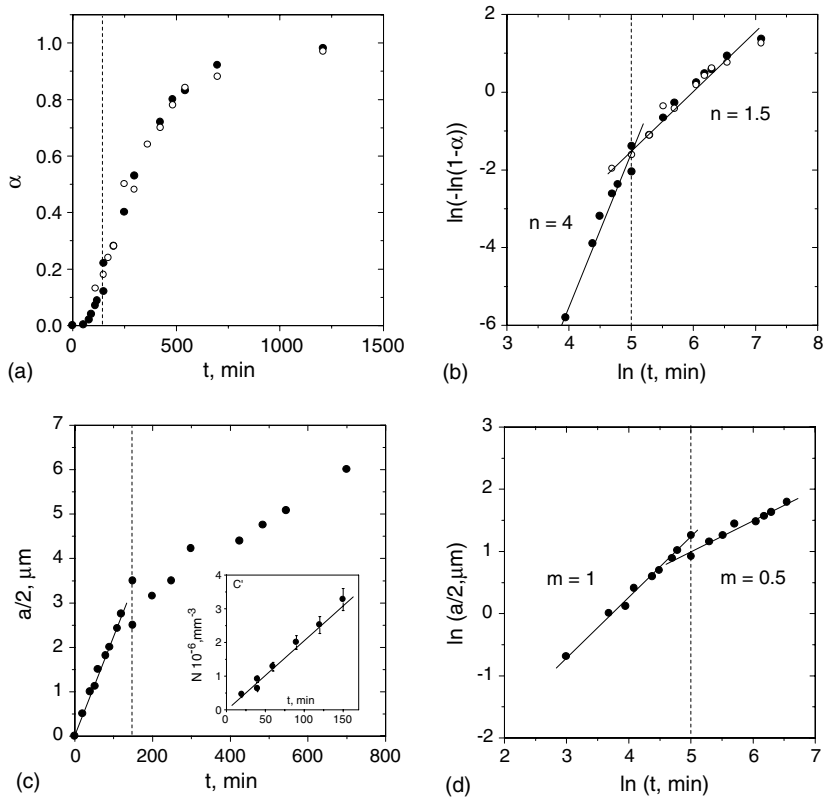

Fig. 6. Volume fraction of crystals (a, b), size of the crystals (c, d), and number of crystals (c′) as functions of the heat treatment time at $T = 647$ °C for glass N5. Open circles – X-ray analysis; closed circles – optical microscopy. Solid lines are linear fit.

with increasing volume fraction of crystals, α, while the contents of silicon and oxygen are constant, within the margins of experimental error. Dotted lines 1 and 2 show the variation of Na and Ca content in the crystals, calculated from the parent glass composition and the glass composition corresponding to different α. Beginning from the early stage of phase transformation, the crystals are enriched with Na in relation to the parent glass and, correspondingly, to the stoichiometric composition. So, as phase transformation proceeds, the crystal composition approaches that of the parent glass. The linear fit of the experimental data for Ca and Na leads us to conclude that, within experimental error, the variation in the crystal composition is accounted for by the replacement of Ca by 2Na. This corresponds to solid solution series between $Na_2O \cdot 2CaO \cdot 3SiO_2$ and $Na_2O \cdot CaO \cdot 2SiO_2$ with the chemical formula $Na_{4+2x}Ca_{4-x}[Si_6O_{18}]$ $(0 \leqslant x \leqslant 1)$ [19].

The initial composition of crystals (nuclei with sizes close to the critical one) is indicated with a black star in Fig. 1. This composition corresponds to $x \approx 0.7$. Open circles show the compositional variation of the glass matrix during crystallization. As we expected, the experimental points are very close to line $Na_2O \cdot SiO_2$–$CaO \cdot SiO_2$. According to [15], the nucleation rate in glasses with compositions close to $Na_2O \cdot 2CaO \cdot 3SiO_2$ is very sensitive to changes in Na_2O content. Fig. 14 shows the nucleation rate in glasses N1–N5 (see Table 1) at $T = 590$ and 650 °C as a function of the sodium content in the original glasses, C_{Na}. Hence, the compositional variation of the glass matrix during crystal growth must affect the nucleation kinetics. Indeed, from the analysis of overall crystallization

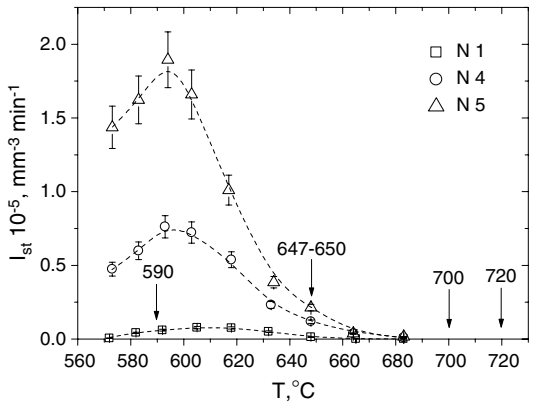

Fig. 7. Steady-state nucleation rates in glasses N1, N4, N5 as functions of temperature [15]. The arrows denote the treatment temperatures used for overall crystallization (see text). Dotted lines are placed just to guide the eye.

(Figs. 2 and 3) presented above, nucleation in glass N4 at $T = 590$ and 650 °C *terminates* at approximately $\alpha \sim 0.2$. This crystallized volume fraction value corresponds approximately to C_{Na} (in the glass matrix) ≈11.5–12 at.% (Figs. 11 and 13). Such a decrease in C_{Na} (for parent glass N4 $C_{Na} = 12.74$ at.%) may suffice to explain the strong drop in the nucleation rate. Although the nucleation rate data (Fig. 14) refer to the glasses of compositions unlike that of the changed by crystal growth (see Fig. 1), the $I(C_{Na})$ plot can be used for a tentative estimation of the nucleation rate change. Thus, according to Fig. 14, the decrease in C_{Na} from 12.7% to 11.5–12 at.% is accompanied by a fivefold to tenfold decrease of the nucleation rate. The distinction between the crystal and glass compositions also leads to a decrease of the crystal growth rate with increasing time (see Figs. 2–6). However, the problem of crystal growth rate variations calls for further investigations.

Figs. 12 and 13 show the compositional variation of crystal and glass due to crystallization at $T = 720$ °C. In general, these variations are analogous to the one at $T = 650$ °C. However, at $T = 650$ °C, the $C_{Na}(\alpha)$ plots are approximately linear up to full crystallization for both crystal and glass (Fig. 11) while, at $T = 720$ °C up to $\alpha \sim 0.8$, C_{Na} in crystals decreases more slowly than at 650 °C, indicating the occurrence of a rapid drop in C_{Na} (Fig. 12). It seems that the difference between 650 and 720 °C is caused mainly by the difference in the average distance, L, between crystals. At $T = 720$ °C, the number of crystals, $N \sim 5000$ mm^{-3}, remains unchanged and corresponds to $L \sim 60$ μm while, at $T = 650$ °C, the number of crystals, for $t \sim 200$ min, reaches the maximal value of $N \geqslant 2 \times 10^6$ mm^{-3}, corresponding to $L \leqslant 8$ μm. Thus, one can expect that the interference (soft impingement of diffusion fields) of the growing crystals, which results from the competition for the available sodium, is fiercer at $T = 650$ °C than at $T = 720$ °C.

The diffusion fields existing around the growing crystals become visible with a second heat treatment at the temperature T_{n-g}, corresponding to reasonable values of nucleation and growth rates. A comparison of the samples subjected to single-stage (Fig. 15(a, c, e)) and double-stage (Fig. 15(b, d, f)) heat treatment reveals that the pre-existing crystals (formed in first heat treatment) strongly reduce the number and size of the crystals nucleated in the following treatment at T_n. In the case of glass N5, no new crystals were formed. Considering the evidence presented above – decreasing sodium content in the glass during phase transformation – it becomes apparent that the areas observed around the large crystals are diffusion fields.

Thus, in the initial stage of phase transformation in both 'stoichiometric' and non-stoichiometric glasses, the compositions of the crystals deviate considerably from those of the parent glasses. From the outset of phase transformation ($\alpha \sim 0$), the sodium content in the crystals exceeds that in the 'stoichiometric' parent glass (N4) by 3–4 at.%, comprising 25–30% of the sodium content in the parent glass! It would therefore appear reasonable that such a difference already exists for critical nuclei in the nucleation stage. However, the deviation of the crystal composition from stoichiometry must diminish the driving force for crystallization. Hence, we must explain why crystals of non-stoichiometric composition nucleate in a stoichiometric glass. It should be noted that the deviation of the crystal composition from that of the fully crystallized glass also takes place in non-stoichiometric glasses (N1, N5).

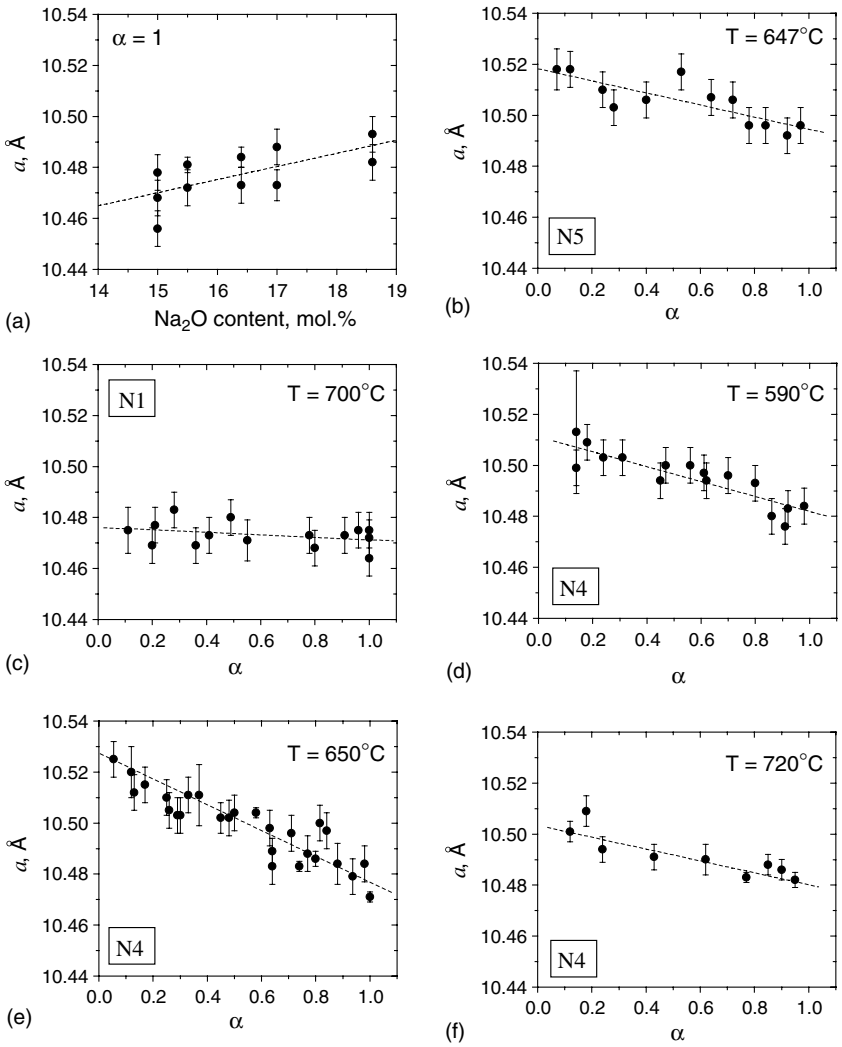

Fig. 8. Parameter ***a*** of the hexagonal crystal cell versus sodium oxide content (a) and volume fraction crystallized (b–f).

According to the CNT, the steady-state homogeneous nucleation rate can be written as

$$I = A \exp\left(-\frac{W^* + \Delta G_D}{kT}\right), \tag{6}$$

where W^* and ΔG_D are the thermodynamic and kinetic barriers for nucleation.

The kinetic barrier is often replaced by the activation free energy for viscous flow ΔG_η. In this approximation, ΔG_D does not depend on the type of crystal. Hence, the nucleation rates of the different thermodynamically possible phases in the same undercooled liquid depend mainly on the thermodynamic barrier. The highest nucleation rate corresponds to the phase having the lowest thermodynamic barrier. However, the thermodynamic barrier includes two main parameters: the crystal/melt surface energy, σ, per unit area of crystal, and the thermodynamic driving force per unit volume of crystal, ΔG_V,

$$W^* = \frac{16\pi}{3}\frac{\sigma^3}{\Delta G_V^2}. \tag{7}$$

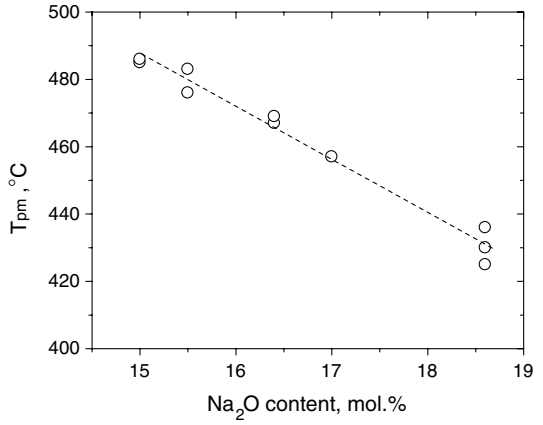

Fig. 9. Temperature of reversible polymorphic transition versus sodium oxide content in fully crystallized glasses.

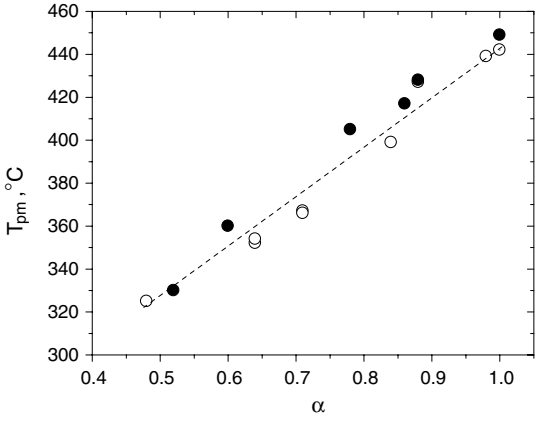

Fig. 10. Temperature of reversible polymorphic transition versus volume fraction crystallized of glass N4. Solid points – dilatometry data; open points – DSC data.

Thus, it is obvious that a decrease in ΔG_V can be compensated for by a decrease in surface energy. It seems that this is the case here. According to analyses of nucleation rates and time lags in glasses N1–N5 performed in [15], within the framework of the CNT, the thermodynamic barrier for nucleation diminishes with increasing sodium content in the glass. If the change of thermodynamic driving force with glass composition is estimated from the variation of liquidus temperature, neglecting the melting entropy

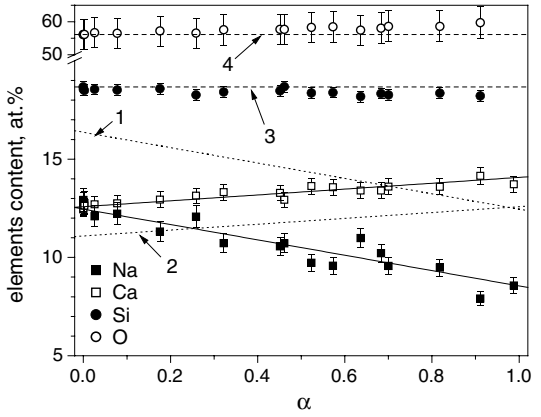

Fig. 11. Composition of glass N4, measured by EDS (points), and of crystals calculated from the parent glass composition (dotted lines 1 and 2 – Na and Ca, respectively) versus volume fraction crystallized at $T = 650$ °C. Solid lines fit the experimental data. Dashed lines 3 (Si) and 4 (O) correspond to the parent glass composition.

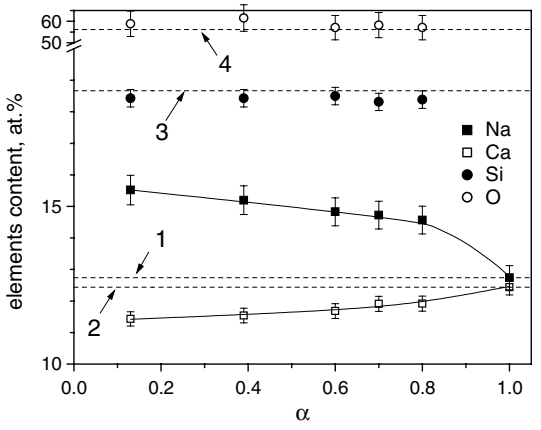

Fig. 12. Composition of crystals in glass N4 measured by EDS versus volume fraction crystallized at $T = 720$ °C. Solid lines are placed just to guide the eye. Dashed lines 1, 2, 3, 4 correspond to the Na, Ca, Si and O contents, respectively, in the parent glass.

change [15], this decrease can be attributed to a decrease of the crystal/melt surface energy.

Here one may draw an analogy to the surface energy on the melt/gas interface. According to Appen [23], replacing calcium oxide by sodium oxide leads to a decrease of the melt/air surface energy of multi-component silicate melts. Thus, we suggest that, due to the decrease in the crystal/melt

Table 2
JMAK equation parameters

Glass	T (°C)	n	m	Comments
N4	590	2.4 ± 0.3	0.8 ± 0.1	Growth of a constant number of crystals: $n \approx 3m$
		1.0 ± 0.1	0.4 ± 0.1	Growth of a constant number of crystals: $n \approx 3m$
	650	4.1 ± 0.3	1.0 ± 0.0	Nucleation and growth at constant rates: $n \approx 1 + 3m$
		1.1 ± 0.1	0.3 ± 0.1	Growth of a constant number of crystals: $n \approx 3m$
	720	1.5 ± 0.1	0.56 ± 0.04	Growth of a constant number of crystals: $n \approx 3m$
N1	700	2.2 ± 0.1	0.69 ± 0.01	Growth of a constant number of crystals: $n \approx 3m$
N5	647	3.8 ± 0.4	0.90 ± 0.06	Nucleation and growth at constant rates: $n \approx 1 + 3m$
		1.5 ± 0.1	0.52 ± 0.04	Growth of a constant number of crystals: $n \approx 3m$

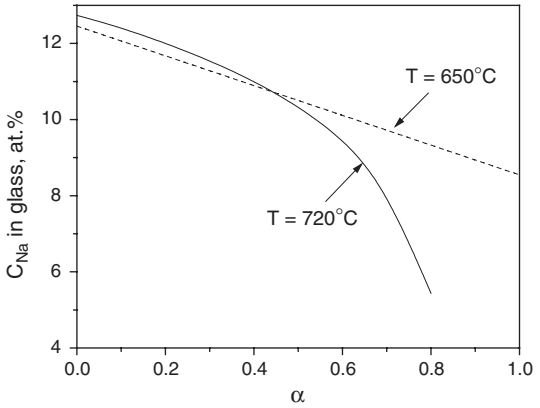

Fig. 13. Sodium content in glass N4 versus volume fraction crystallized at 720 °C (calculated from the data of Fig. 12) and 650 °C (linear fit of direct measurements presented in Fig. 11).

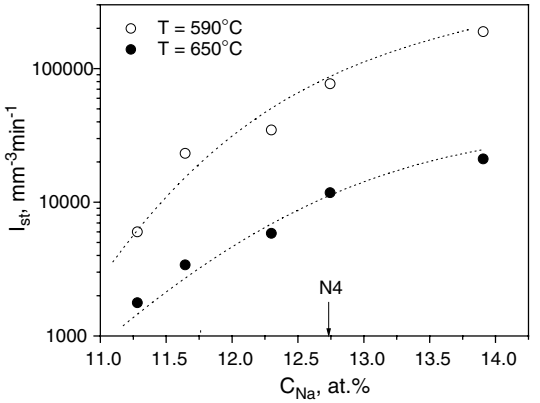

Fig. 14. Nucleation rates at 590 and 650 °C as functions of the sodium content in the parent glasses. Dotted lines are placed just to guide the eye. Arrow marks sodium content in glass N4.

surface energy, sodium-rich solid solution crystals have a lower thermodynamic barrier (higher nucleation rate) than stoichiometric crystals.

The proposed explanation is consistent with Ostwald's generalized rule of stages [24], according to which "In phase transformation processes, the structure and properties of the critical nucleus may differ qualitatively from the properties both of the ambient and of the newly evolving macrophases. Those classes of critical clusters determine the process of the transformation, which correspond to a minimum of the work of critical cluster formation (as compared with all other possible alternative structures and compositions, which may be formed at the given thermodynamic constraints)".

The growth of sodium-enriched crystals is problematic owing to the depletion of sodium in the glass matrix. When the diffusion zones surrounding the crystals impinge, the solid solution crystals are forced to change their composition, approaching the glass composition. In the final stages of phase transformation, the average composition of crystals equals that of the parent glass.

Let us recall that the CNT fails to quantitatively describe nucleation rates in glasses. If one assumes a constant nucleus/liquid surface energy, drastic discrepancies result between theoretical and experimental nucleation rates [25]. Since the formation of solid solution is typical for silicate systems, it is important to keep in mind that the composition of the critical nuclei and, correspondingly, their thermodynamic driving force and surface energy may differ considerably from those of the final macrophase. According to the data presented here, even stoichiometric crystals can form

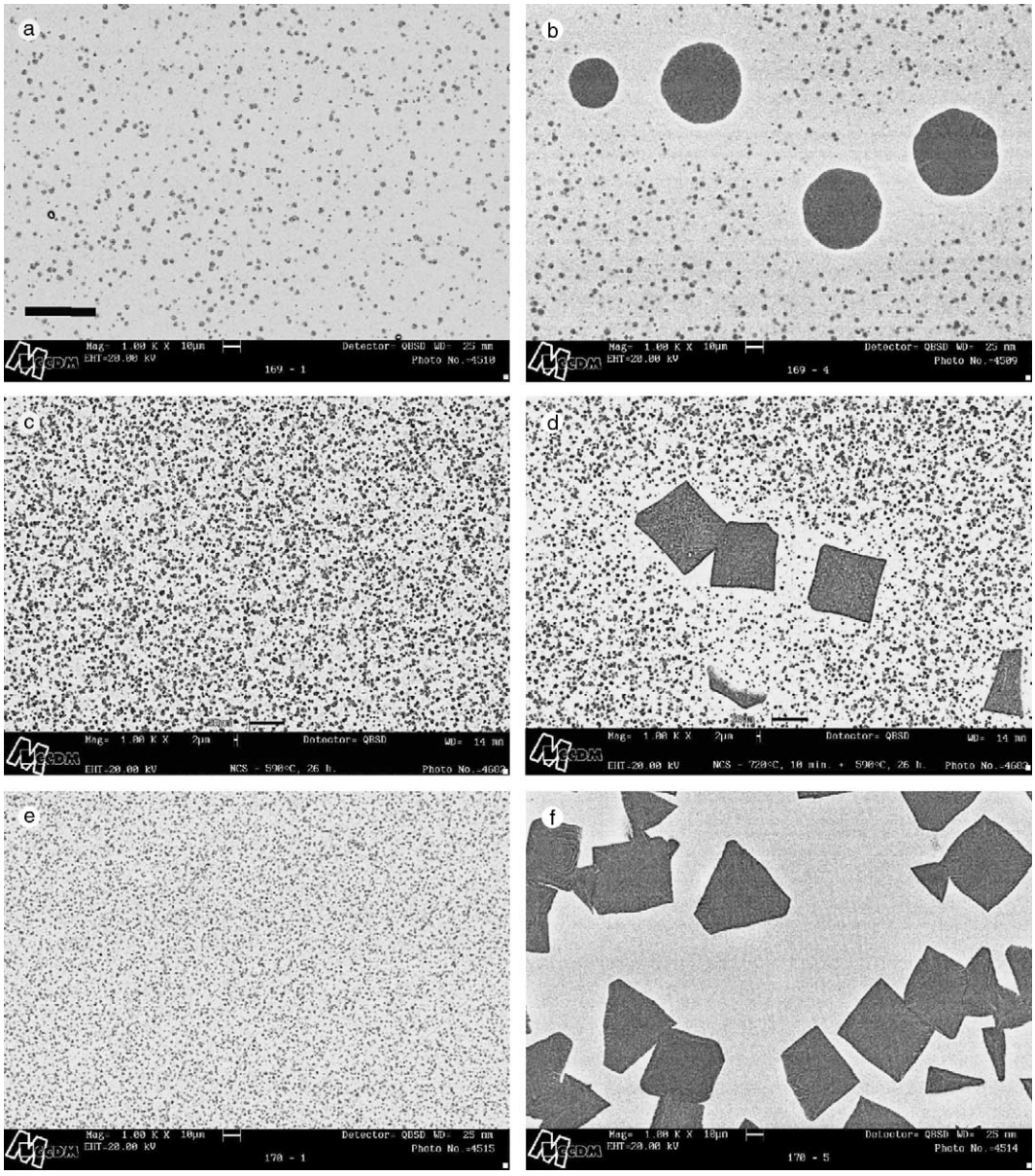

Fig. 15. SEM micrographs of glasses N1, N4 and N5 subjected to single (a, c, e) and double stage (b, d, f) heat treatments. Single stage: T_{n-g}, t_{n-g}; double stage: T_{gr}, $t_{gr} + T_{n-g} \cdot t_{n-g}$; $T_{n-g} = 590$ °C; $t_{n-g} = 1340$ min (a), 1560 min (c), 2140 min (e). $T_{gr} = 700$ °C (b), 720 °C (d, f); $t_{gr} = 40$ min (b), 10 min (d), 20 min (f). Bar denotes 50 μm.

through the nucleation of solid solutions. Thus, the deviation of the nuclei composition from the expected one may have a significant impact on analyses of nucleation theories.

A formal analysis using CNT shows that if a diminished driving force is allowed for, the discrepancy between theoretical predictions and experimental nucleation data is reduced [26]. The decrease in driving force may be caused by elastic strain, metastable phase formation, or continuous changes in nuclei composition (shown in this paper). Hence, it is possible that the use of the

proper thermodynamic driving force for non-stoichiometric critical nucleus formation (instead of the classical assumption of stoichiometric nucleus formation, which is equal to the final macrophase) may partly explain the CNT's failure. It is thus necessary to generalize (or not) the present findings with other compositions.

5. Conclusions

In the early stages of crystallization, the composition of sodium-rich solid solution crystals and, inferentially, of critical nuclei, deviates considerable from that of the parent glass in both stoichiometric ($Na_2O \cdot 2CaO \cdot 3SiO_2$) and slightly non-stoichiometric glasses, but gradually approaches it as crystallization proceeds. The existence of such mutant crystals is reported for the first time.

The thermodynamic barrier for nucleation decreases with increased sodium content in the crystals likely owing to a decrease in nucleus/liquid interfacial energy. This is the kinetic reason for the nucleation of sodium-rich crystals. These crystals are surrounded by sodium-depleted diffusion fields, which can be visualized by performing a second heat treatment at a lower temperature corresponding to reasonable nucleation and growth rate values. The change in the glass composition during crystallization causes the termination of nucleation and a decrease in the crystal growth rate.

The deviation of the nucleus composition from the expected stoichiometry may have a significant impact on the analysis of nucleation theories.

Acknowledgements

The authors gratefully acknowledge helpful discussions with Drs B.A. Shakhmatkin and M.O. Prado. The funding provided by CNPq, Pronex, Cyted and Fapesp (Brazil) is deeply appreciated.

References

[1] W. Ostwald, Z. Phys. Chem. 22 (1897) 289.
[2] J. Deubener, R. Brückner, M. Sternitzke, J. Non-Cryst. Solids 163 (1993) 1.
[3] E.D. Zanotto, M.L.G. Leite, J. Non-Cryst. Solids 202 (1996) 145.
[4] Y. Iqbal, W.E. Lee, D. Holland, P.F. James, J. Non-Cryst. Solids 224 (1998) 1.
[5] L.L. Burgner, P. Lucas, M.C. Weinberg, P.C. Soares Jr., E.D. Zanotto, J. Non-Cryst. Solids 274 (2000) 188.
[6] L.L. Burgner, M.C. Weinberg, P. Lucas, P.C. Soares Jr., J. Non-Cryst. Solids 255 (1999) 264.
[7] V.N. Filipovich, A.M. Kalinina, Inorg. Mater. 4 (4) (1968) 1532.
[8] M. Ito, T. Sakaino, T. Moriya, Bull. Tokyo Inst. Technol. (88) (1968) 127.
[9] V.M. Fokin, A.M. Kalinina, V.N. Filipovich, J. Cryst. Growth 52 (1981) 115.
[10] E.D. Zanotto, P.F. James, J. Non-Cryst. Solids 74 (1985) 373.
[11] J.W.P. Schmelzer, R. Müller, J. Möller, I.S. Gutzow, Phys. Chem. Glasses 43C (2002) 291.
[12] J.W.P. Schmelzer, R. Müller, J. Möller, I.S. Gutzow, J. Non-Cryst. Solids 315 (2003) 144.
[13] C.J.R. Gonzalez-Oliver, P.F. James, J. Non-Cryst. Solids 38&39 (1980) 699.
[14] K. Lakshmi Narayan, K.F. Kelton, J. Non-Cryst. Solids 220 (1997) 222.
[15] O.V. Potapov, V.M. Fokin, V.L. Ugolkov, L.Y. Suslova, V.N. Filipovich, Glass Phys. Chem. 26 (2000) 39.
[16] V.M. Fokin, O.V. Potapov, C.R. Chinaglia, E.D. Zanotto, J. Non-Cryst. Solids 258 (1999) 180.
[17] E.D. Zanotto, A. Galhardi, J. Non-Cryst. Solids 104 (1988) 73.
[18] G.K. Moir, F.P. Glasser, Phys. Chem. Glasses 15 (1) (1974) 6.
[19] I. Maki, T. Sugimura, J. Ceram. Assoc. Jpn. 76 (5) (1968) 144.
[20] H. Ohsato, Y. Takeuchi, I. Maki, Acta Cryst. B46 (1990) 125.
[21] D. Kashchiev, Nucleation. Basic Theory and Applications, Butterworth, Heinemann, 2000.
[22] J.W. Christian, The Theory of Transformation in Metals and Alloys, Part I, Pergamon, Oxford, 1981.
[23] J.M.F. Navarro, El vidrio, Spain, 1991.
[24] J.W.P. Schmelzer, I. Gutzow, J. Schmelzer Jr., J. Chem. Phys. 112 (2000) 3820.
[25] E.D. Zanotto, V.M. Fokin, Philos. Trans. R. Soc., Ser. A 361 (2003) 591.
[26] V.M. Fokin, E.D. Zanotto, unpublished data.